

Supporting Information (SI)

Accelerated discovery of thermostable high-energy material with intramolecular donor-acceptor building blocks

Qing Ma[†], Zhen Cheng[†], Lei Yang[†], Wei Du, Yilin Yin, Wenqiang Ma, Guijuan Fan*,

Jinshan Li*

Institute of Chemical Materials, China Academy of Engineering Physics, Mianyang 621900,
China.

* Corresponding authors (emails: fangj609@caep.cn (Fan G); ljs915@263.net (Li J))

[†]These authors contributed equally to this work.

Table of contents

1 Experimental section	3
2 Crastallographic date for NTTO ·DMF and NTTO ·DMSO solvates	6
3 Theoretical study	14
4 References	14
5 ¹ H and ¹³ C NMR spectra of NTTO	15
6 FT-IR spectra of NTTO	16

1 Experimental section

General methods

^1H and ^{13}C NMR spectra were recorded on 500 MHz (Bruker AVANCE 500) nuclear magnetic resonance spectrometers operating at 500 and 125 MHz, respectively, by using DMSO- d_6 as the solvent and locking solvent unless otherwise stated. Chemical shifts in ^1H and ^{13}C spectra are reported relative to DMSO. DSC was performed at a heating rate of $10\text{ }^\circ\text{C min}^{-1}$ in closed Al containers with a nitrogen flow of 20 mL min^{-1} on an STD-Q600 instrument. Infrared (IR) spectra were recorded on a Perkin-Elmer Spectrum BX FT-IR equipped with an ATR unit at $25\text{ }^\circ\text{C}$. Impact sensitivity, friction sensitivity and electrostatic discharge sensitivity of samples are measured by using the standard BAM methods. The experimental density was determined by helium pycnometry and a Micromeritics AccuPyc II 1340 device at the ambient temperature.

X-ray crystallography

The data were collected with a Bruker three-circle platform diffractometer equipped with a SMART APEX II CCD detector. A Kryo-Flex low-temperature device was used to keep the crystals at a constant 298 K during the data collection. The data collection and the initial unit cell refinement were performed by using APEX2 (v2010.3-0). Data reduction was performed by using SAINT (v7.68A) and XPREP (v2008/2). Corrections were applied for Lorentz, polarization, and absorption effects by using SADABS (v2008/1). The structure was solved and refined with the aid of the programs in the SHELXTL-plus (v2008/4) system of programs. The full-matrix least-squares refinement on F2 included atomic coordinates and anisotropic thermal parameters for all non-H atoms. The H atoms were included in a riding model. The structure was solved by direct methods with SHELXS-97 and expanded by using the Fourier technique. The nonhydrogen atoms were refined anisotropically. The hydrogen atoms were located and refined.

Combinatorial data search and intramolecular stabilization design.

We began the search for fused triazolotriazine scaffolds involving 0%-100% similarity in the SciFinder database to get 4617 fused scaffolds. Subsequently, after the similarity was restricted to 60%, 708 scaffolds were obtained during the process of “deep bed” filtration. In order to design energetic materials, the nitro group was introduced, 451 fused scaffolds were acquired afterwards. To further discover the

desired energetic materials, we used the workflow of molecular design which was illustrated in the right side of Figure 1. Four positions in the triazolotriazine framework could be substituted with energetic groups (-N₃, -NO₂, -N₄O₈ (gem-dinitro), -CN₄ (tetrazole), N-O (N-oxide), -NHNO₂, -NH₂, etc), which aimed to narrow the scope by eliminating the scaffolds with nonconforming structures. In the next key step, we used an intramolecular stabilization approach for material selection, meaning there must be at-least one intramolecular hydrogen bonds in these fused triazolotriazine energetic materials. Following this restraint condition, only 16 candidates were found out as demonstrated in Figure 2. Those candidates show at least one intramolecular donor-acceptor building block. To meet the experimental requirements, HB>1 is necessary. After analyzing the experimental feasibility of the remaining ones, we assumed that **C4**, **C8**, **C12**, **C14~C16** owning two intramolecular hydrogen bonds should have superior comprehensive performance to others. When we searched those candidates, we found that **C1**, **C2**, **C3**, **C13** had been reported. **C1** and **C13** showed higher thermal stability (246 °C, 290°C) but **C3** presented lower density (1.67 g cm⁻³), **C2** and **C3** exhibited higher densities (1.87 cm⁻³, 1.90 g cm⁻³) but lower stability (138 °C, 181°C). Therefore, **C4** was more realizable because there might exist one step synthesis from **C3**.

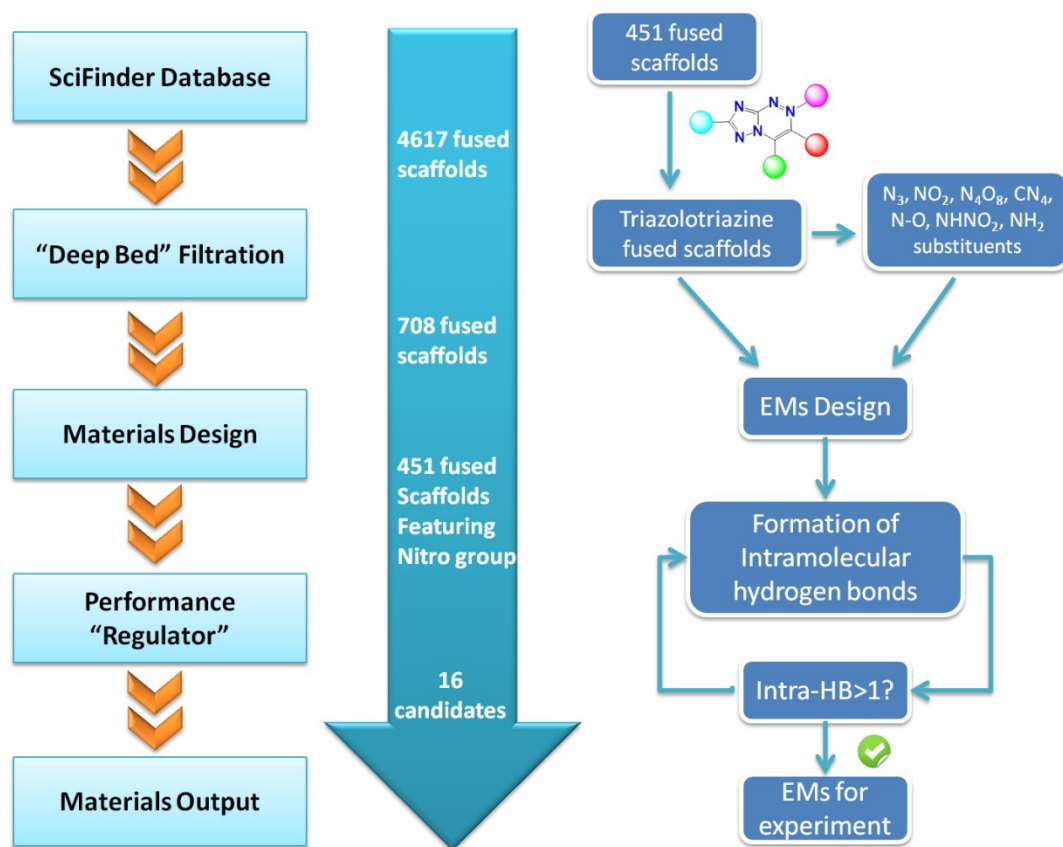
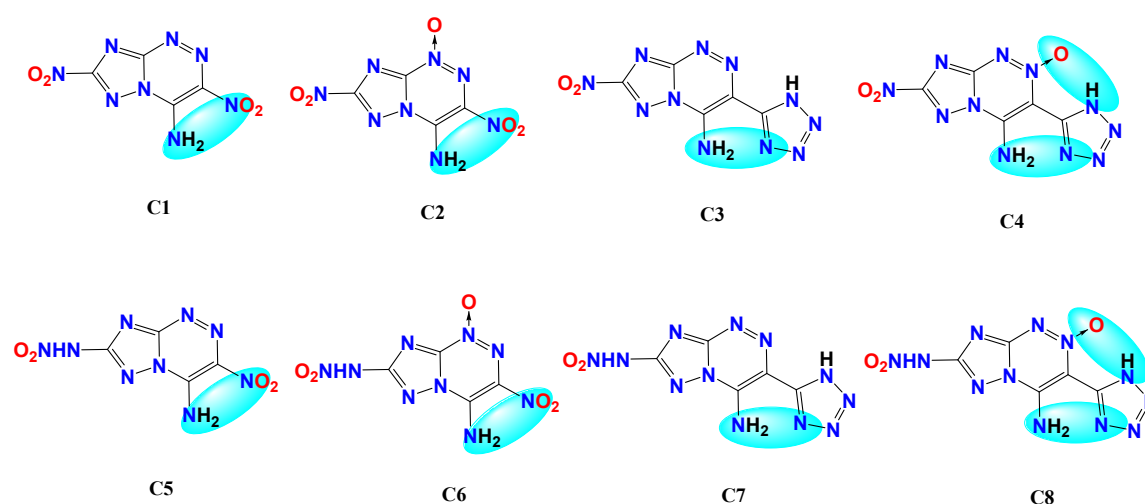


Fig.S1 Workflow of current investigation and diagram for how to obtain the thermostable fused triazolotriazine EMs.



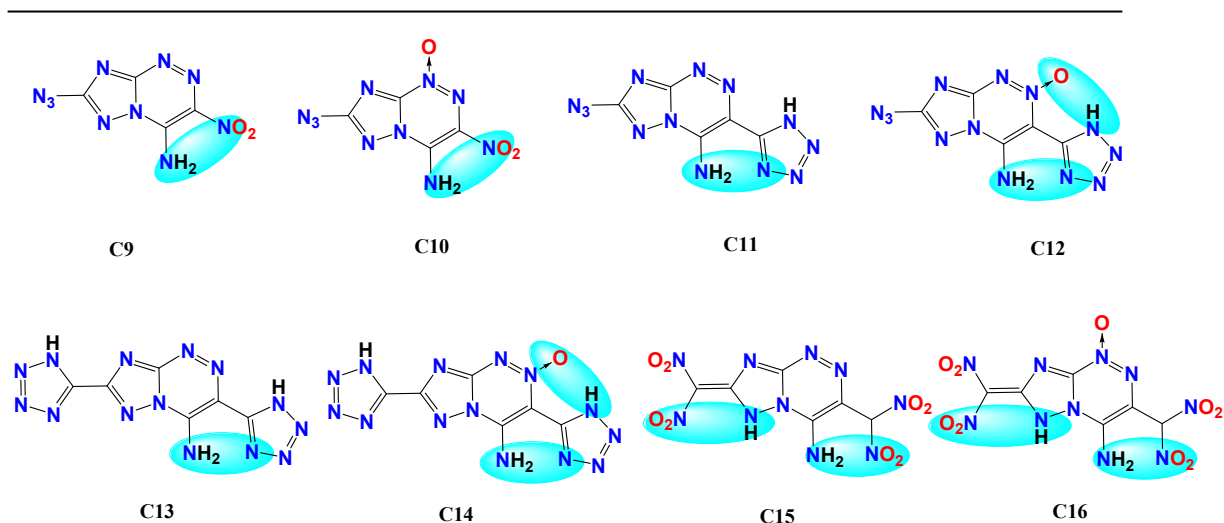


Fig.S2 Fused triazole-triazine energetic materials candidates with at least one donor-acceptor building block (blue bar).

Synthesis of 7-nitro-3-(1H-tetrazol-5-yl)-[1,2,4]triazolo[5,1-c][1,2,4]triazin-4-amine-2-oxide (C4, NTTO).

C 3 (1.245 g, 5.0 mmol) was added in portions to a mixture of 50% H₂O₂ (6.0 mL) and TFAA (10 mL) at 0 °C, and then stirred for 8 hours at room temperature. The reaction mixture was poured into ice-water, the yellow precipitate was filtered, washed with water, and dried in air to afford energetic material **NTTO** (1.167 g, 88.1 %). ¹H NMR: δ = 10.82 (s, 1H), 9.75 (s, 2H). ¹³C NMR: δ = 164.46, 154.23, 147.26, 146.47, 110.17 ppm. IR: $\tilde{\nu}$ = 3450, 3217, 1664, 1592, 1562, 1478, 1404, 1360, 1322, 1274, 1236, 1198, 1173, 1099, 1073, 1022, 899, 840, 752 cm⁻¹. Elemental analysis (EA) of C₅H₃N₁₁O₃ (265.15): calcd C, 22.65; H, 1.14; N, 58.11 %. Found: C 21.94, H 1.18, N 58.65 %.

2 Crystallographic data for NTTO

Table S1. Crystal data and details of the structure determination

	C ₅ H ₃ N ₁₁ O ₃ ·DMSO·H ₂ O 2(C ₅ H ₃ N ₁₁ O _{2.5})·2(DMF)·2(H ₂ O)	
CCDC number	2117393	2117394
Empirical formula	C ₇ H ₁₁ N ₁₁ O ₅ S	C ₁₆ H ₂₄ N ₂₄ O ₉

Formula weight	361.33	696.59
Temperature/K	170	115
Crystal system	triclinic	triclinic
Space group	P-1	P-1
a/Å	5.5300(8)	6.7298(3)
b/Å	17.308(3)	6.9801(4)
c/Å	29.896(4)	15.5552(7)
α/°	85.857(6)°	77.956(2)
β/°	86.344(4)°	82.164(2)
γ/°	88.325(5)°	89.214(2)
Volume/Å³	2847.3(8)	707.86(6)
Z	8	1
ρ_{calc}/cm³	1.686	1.634
μ/mm⁻¹	0.280	0.136
F(000)	1488.0	360.0
Crystal size/mm³	0.12×0.08× 0.05	0.15×0.08× 0.05
Radiation	MoKα(λ= 0.71073)	MoKα(λ= 0.71073)
2θ range for data collection/°	4.106 to 50.994	5.406 to 52.87
Index ranges	-6 ≤ h ≤ 6, -20 ≤ k ≤ 20, - 36 ≤ l ≤ 35	-8 ≤ h ≤ 7, -8 ≤ k ≤ 8, -19 ≤ l ≤ 18
Reflections collected	29326	8216
Independent reflections	10458 [R _{int} = 0.0977, R _{sigma} = 0.1345]	2889 [R _{int} = 0.0404, R _{sigma} = 0.0451]
Data/restraints/parameters	10458/1/886	2889/210/240
Goodness-of-fit on F²	1.024	1.099
Final R indexes [I ≥ 2σ (I)]	R ₁ = 0.0864, wR ₂ = 0.1894	R ₁ = 0.0491, wR ₂ = 0.1134
Final R indexes [all data]	R ₁ = 0.1831, wR ₂ = 0.2458	R ₁ = 0.0622, wR ₂ = 0.1219

Largest diff. peak/hole / e Å⁻³

0.75/-0.85

0.27/-0.32

Table S2. Bond Lengths for **NTTO·DMSO**

Atom	Atom	Length/Å	Atom	Atom	Length/Å
S001	O6	1.512(5)	N15	N12	1.355(7)
S001	C25	1.781(7)	N15	C6	1.331(8)
S001	C26	1.774(7)	O10	N28	1.213(7)
S002	O15	1.511(5)	N10	C3	1.312(8)
S002	C22	1.744(9)	N23	N24	1.333(7)
S002	C21	1.772(8)	N23	C14	1.383(8)
S003	O14	1.520(5)	N20	C10	1.312(8)
S003	C27	1.786(10)	N18	C9	1.327(8)
S003	C28	1.611(11)	N1	N2	1.353(8)
S004	O18	1.521(5)	N1	C5	1.338(8)
S004	C24	1.714(10)	N43	C19	1.328(8)
S004	C23	1.796(10)	O17	N41	1.228(7)
O19	N44	1.238(7)	N26	N27	1.406(8)
O12	N23	1.250(7)	N26	C11	1.359(8)
O3	N5	1.262(7)	N26	C13	1.355(8)
O7	N17	1.256(7)	N40	C20	1.316(8)
O9	N22	1.227(7)	O11	N28	1.225(8)
O2	N11	1.215(7)	N35	N36	1.309(8)
N9	N8	1.363(7)	N24	C11	1.336(9)
N9	C2	1.376(8)	N27	C12	1.330(8)
N9	C3	1.374(8)	N8	C1	1.324(8)
O8	N22	1.229(7)	N12	N13	1.297(7)
N16	C8	1.322(7)	N13	N14	1.335(7)

N19	N20	1.363(7)	N14	C6	1.335(8)
N19	C8	1.364(8)	N25	C11	1.338(9)
N19	C9	1.384(8)	N25	C12	1.334(9)
N39	N40	1.354(7)	N2	N3	1.316(8)
N39	C19	1.377(8)	N4	N3	1.329(7)
N39	C16	1.371(8)	N4	C5	1.338(8)
N44	N43	1.342(7)	N41	C20	1.465(9)
N44	C17	1.391(7)	N30	N31	1.349(8)
N6	N5	1.327(7)	N30	C15	1.328(9)
N6	C2	1.333(8)	N37	N36	1.338(7)
O16	N41	1.215(7)	N37	C18	1.323(8)
N21	C9	1.326(8)	N11	C1	1.443(9)
N21	C10	1.342(8)	N28	C12	1.446(9)
N38	C16	1.308(8)	N33	N32	1.384(8)
N17	N18	1.330(7)	N33	C15	1.339(9)
N17	C7	1.399(8)	C8	C7	1.401(9)
N7	C2	1.329(9)	N29	C13	1.317(8)
N7	C1	1.334(8)	N32	N31	1.290(8)
N22	C10	1.457(9)	C7	C6	1.435(9)
O1	N11	1.226(7)	C4	C3	1.397(9)
N5	C4	1.379(8)	C4	C5	1.447(9)
N34	N35	1.348(7)	C18	C17	1.459(9)
N34	C18	1.323(8)	C17	C16	1.408(9)
N42	C19	1.317(8)	C14	C15	1.432(9)
N42	C20	1.341(8)	C14	C13	1.404(10)

Table S3. Bond Angles for **NTTO·DMSO**.

Atom	Atom	Atom	Angle/	Atom	Atom	Atom	Angle/
------	------	------	--------	------	------	------	--------

O6	S001	C25	106.3(3)	N35	N36	N37	105.6(5)
O6	S001	C26	104.6(3)	O10	N28	O11	125.2(7)
C26	S001	C25	97.4(4)	O10	N28	C12	117.3(6)
O15	S002	C22	106.6(4)	O11	N28	C12	117.4(6)
O15	S002	C21	105.3(4)	N2	N3	N4	106.6(6)
C22	S002	C21	97.4(5)	C15	N33	N32	105.7(6)
O14	S003	C27	105.9(4)	N16	C8	N19	118.3(6)
O14	S003	C28	100.4(4)	N16	C8	C7	127.4(6)
C28	S003	C27	99.7(5)	N19	C8	C7	114.3(5)
O18	S004	C24	103.9(4)	N31	N32	N33	109.3(6)
O18	S004	C23	105.5(4)	N17	C7	C8	119.7(6)
C24	S004	C23	97.5(5)	N17	C7	C6	119.1(6)
N8	N9	C2	111.1(5)	C8	C7	C6	121.1(5)
N8	N9	C3	126.9(5)	N21	C9	N19	109.0(6)
C3	N9	C2	122.0(6)	N21	C9	N18	126.8(6)
N20	N19	C8	126.7(5)	N18	C9	N19	124.2(6)
N20	N19	C9	110.9(5)	N5	C4	C3	120.2(6)
C8	N19	C9	122.3(5)	N5	C4	C5	119.9(6)
N40	N39	C19	111.2(5)	C3	C4	C5	120.0(6)
N40	N39	C16	126.1(5)	N6	C2	N9	123.9(6)
C16	N39	C19	122.6(6)	N7	C2	N9	109.0(6)
O19	N44	N43	117.2(5)	N7	C2	N6	127.1(6)
O19	N44	C17	119.5(5)	N34	C18	N37	108.1(5)
N43	N44	C17	123.3(6)	N34	C18	C17	122.2(6)
N5	N6	C2	114.6(5)	N37	C18	C17	129.6(6)
C9	N21	C10	100.9(5)	N15	C6	N14	107.1(6)
O7	N17	N18	117.2(5)	N15	C6	C7	122.4(6)
O7	N17	C7	117.9(5)	N14	C6	C7	130.5(6)

N18	N17	C7	124.9(6)	N44	C17	C18	118.4(6)
C2	N7	C1	101.3(5)	N44	C17	C16	121.0(6)
O9	N22	O8	124.1(6)	C16	C17	C18	120.5(6)
O9	N22	C10	119.0(5)	N9	C3	C4	114.2(6)
O8	N22	C10	116.9(6)	N10	C3	N9	118.4(6)
O3	N5	N6	116.1(5)	N10	C3	C4	127.4(6)
O3	N5	C4	118.7(6)	N42	C19	N39	109.4(6)
N6	N5	C4	125.1(6)	N42	C19	N43	126.8(6)
C18	N34	N35	106.1(5)	N43	C19	N39	123.9(6)
C19	N42	C20	100.7(5)	N39	C16	C17	113.6(6)
C6	N15	N12	106.3(5)	N38	C16	N39	119.1(6)
O12	N23	N24	116.5(5)	N38	C16	C17	127.2(6)
O12	N23	C14	119.1(6)	N1	C5	C4	122.7(6)
N24	N23	C14	124.4(6)	N4	C5	N1	107.8(6)
C10	N20	N19	98.8(5)	N4	C5	C4	129.5(6)
C9	N18	N17	114.5(5)	N32	N31	N30	107.9(6)
C5	N1	N2	106.0(5)	N23	C14	C15	119.7(7)
C19	N43	N44	115.5(5)	N23	C14	C13	120.1(6)
C11	N26	N27	110.3(6)	C13	C14	C15	120.3(6)
C13	N26	N27	126.6(6)	N24	C11	N26	123.7(6)
C13	N26	C11	123.1(6)	N24	C11	N25	126.2(6)
C20	N40	N39	98.5(5)	N25	C11	N26	110.0(6)
N36	N35	N34	110.5(5)	N21	C10	N22	120.7(5)
N23	N24	C11	114.7(6)	N20	C10	N21	120.3(6)
C12	N27	N26	98.3(6)	N20	C10	N22	119.0(6)
C1	N8	N9	98.7(5)	N42	C20	N41	120.7(6)
N13	N12	N15	110.6(5)	N40	C20	N42	120.2(6)
N12	N13	N14	106.1(5)	N40	C20	N41	119.1(6)

N13	N14	C6	109.9(5)	N27	C12	N25	119.9(7)
C12	N25	C11	101.5(6)	N27	C12	N28	117.6(7)
N3	N2	N1	110.2(5)	N25	C12	N28	122.5(6)
N3	N4	C5	109.5(6)	N7	C1	N11	121.8(6)
O16	N41	O17	125.1(6)	N8	C1	N7	119.9(7)
O16	N41	C20	118.0(6)	N8	C1	N11	118.3(6)
O17	N41	C20	116.9(6)	N30	C15	N33	108.5(6)
C15	N30	N31	108.6(6)	N30	C15	C14	129.2(7)
C18	N37	N36	109.7(5)	N33	C15	C14	122.4(7)
O2	N11	O1	124.8(6)	N26	C13	C14	114.0(6)
O2	N11	C1	117.3(6)	N29	C13	N26	118.3(7)
O1	N11	C1	117.9(6)	N29	C13	C14	127.6(6)

Table S4. Bond Lengths for **NTTO·DMF**

Atom	Atom	Length/Å	Atom	Atom	Length/Å
O5	C8	1.240(3)	N10	C4	1.334(3)
O3	N11	1.219(3)	N10	C5	1.337(3)
O4	N11	1.220(2)	N6	N7	1.329(2)
N8	N9	1.367(2)	N6	C2	1.355(3)
N8	C3	1.366(3)	N6	O1	1.160(4)
N8	C4	1.372(3)	N12	C8	1.321(3)
N5	C3	1.316(3)	N12	C6	1.458(3)
N4	N3	1.341(2)	N12	C7	1.455(3)
N4	C1	1.339(3)	N7	C4	1.337(3)
N1	N2	1.357(2)	N11	C5	1.463(3)
N1	C1	1.331(3)	C3	C2	1.406(3)
N9	C5	1.327(3)	C2	C1	1.455(3)
N2	N3	1.304(2)			

Table S5. Bond Angles for **NTTO·DMF**.

Atom	Atom	Atom	Angle/	Atom	Atom	Atom	Angle/
N9	N8	C4	111.14(16)	O4	N11	C5	116.80(19)
C3	N8	N9	126.03(17)	N8	C3	C2	112.58(17)
C3	N8	C4	122.82(17)	N5	C3	N8	119.63(18)
C1	N4	N3	108.31(17)	N5	C3	C2	127.79(18)
C1	N1	N2	105.33(16)	N6	C2	C3	122.37(18)
C5	N9	N8	98.61(17)	N6	C2	C1	116.50(18)
N3	N2	N1	110.79(16)	C3	C2	C1	121.12(18)
C4	N10	C5	100.96(17)	N10	C4	N8	109.30(18)
N7	N6	C2	123.64(18)	N10	C4	N7	127.46(19)
O1	N6	N7	110.8(2)	N7	C4	N8	123.23(19)
O1	N6	C2	125.5(3)	N4	C1	C2	127.37(19)
N2	N3	N4	106.72(16)	N1	C1	N4	108.85(17)
C8	N12	C6	121.89(19)	N1	C1	C2	123.77(18)
C8	N12	C7	121.14(19)	N9	C5	N10	119.98(19)
C7	N12	C6	116.97(18)	N9	C5	N11	118.49(19)
N6	N7	C4	115.36(17)	N10	C5	N11	121.51(19)
O3	N11	O4	126.03(19)	O5	C8	N12	125.4(2)
O3	N11	C5	117.16(18)				

3 Theoretical study

Theoretical calculations were performed by using the Gaussian 09 (Revision D.01) suite of programs.^[1] The elementary geometric optimization and the frequency analysis were performed at the level of the Becke three parameter, Lee-Yan-Parr (B3LYP) functional with the 6-311+G** basis set.^[2] All of the optimized structures were characterized to be local energy minima on the potential surface without any imaginary frequencies. Atomization energies were calculated by the CBS-4M.^[3] All

the optimized structures were characterized to be true local energy minima on the potential-energy surface without imaginary frequencies.^[4]

The predictions of heat of formation (*HOF*) adopt the hybrid DFT-B3LYP methods with 6-311+G** basis set via designed isodesmic reactions. The isodesmic reaction processes, i.e., the number of each kind of formal bond is conserved, are used with application of the bond separation reaction (BSR) rules. The molecule is broken down into a set of two heavy-atom molecules containing the same component bonds. The isodesmic reactions used to derive the HOF of the title compounds are in Scheme S1. The change of enthalpy for the reactions at 298 K can be expressed as

$$\Delta H_{298} = \sum \Delta_f H_P - \sum \Delta_f H_R \quad (1)$$

Where $\sum \Delta_f H_P$ and $\sum \Delta_f H_R$ are the HOF of reactants and products at 298 K, respectively, and ΔH_{298} can be calculated using the following expression

$$\Delta H_{298} = \Delta E_{298} + \Delta(PV) = \Delta E_0 + \Delta ZPE + \Delta H_T + \Delta nRT \quad (2)$$

Where ΔE_0 is the change in total energy between the products and the reactants at 0 K; ΔZPE is the difference between the zero-point energies (ZPE) of the products and the reactants at 0 K; ΔH_T is thermal correction from 0 to 298 K. The $\Delta(PV)$ value in Eq. (2) is the PV work term. It equals $\Delta(nRT)$ for the reactions of ideal gas. For the isodesmic reaction, $\Delta n = 0$, so $\Delta(PV) = 0$. On the left side of Eq. (1), apart from target compound, all the others are called reference compounds. The HOF of reference compounds is available from the experiments.

4 References

- [1] Frisch MJ, Trucks GW, Schlegel HB, Daniels AD, Farkas O, Foresman JB, Ortiz JV, Cioslowski J, Fox DJ. Gaussian 09, Revision D. 01, Gaussian, Inc. Wallingford CT, 2009.
- [2] Hariharan PC, Pople JA, Influence of polarization functions on MO hydrogenation energies, *Theor Chim Acta*. 1973; 28, 3, 213-222.
- [3] Ochterski JW, Petersson GA, Montgomery JA, Lattice dynamics and hyperfine interactions of $C_{60}Fe(CO)_4$, *J Chem Phys*. 1996; 104, 7, 2598-2619.
- [4] Jenkins HDB, Tudeal D, Glasser L, Lattice potential energy estimation for complex ionic salts from density measurements, *Inorg Chem*. 2002; 41, 9, 2364-2367.

5 ^1H and ^{13}C NMR spectra of NTTO

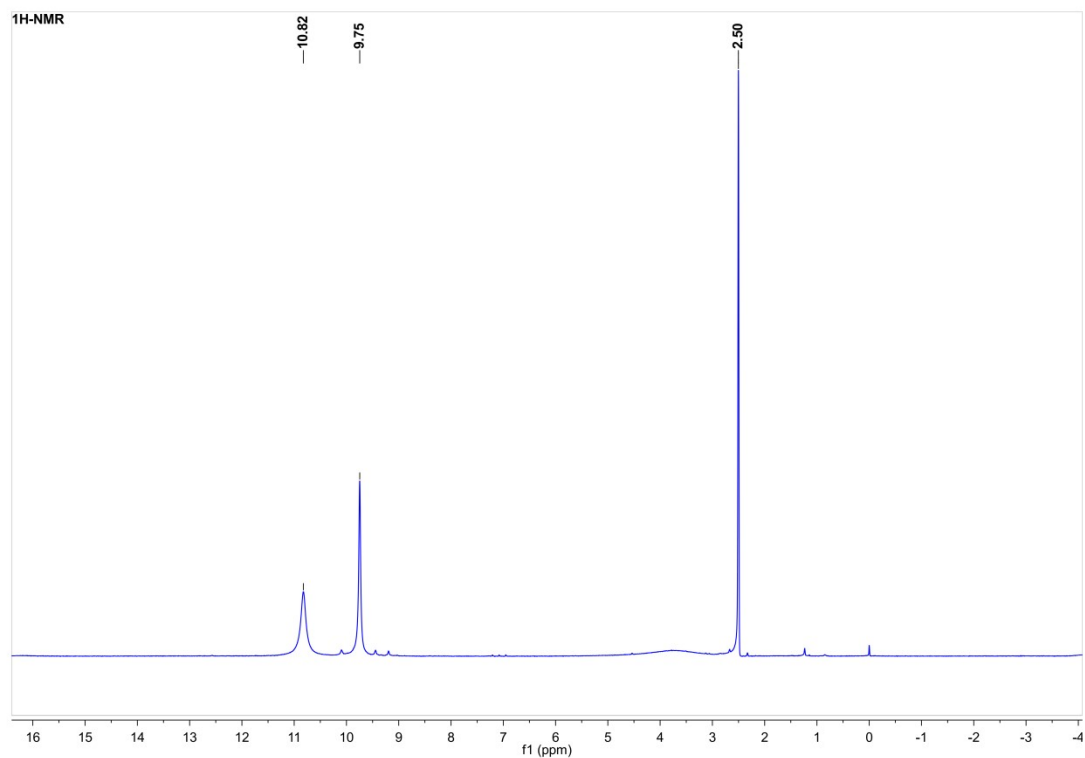


Fig. S3 ^1H NMR of NTTO (DMSO-d₆)

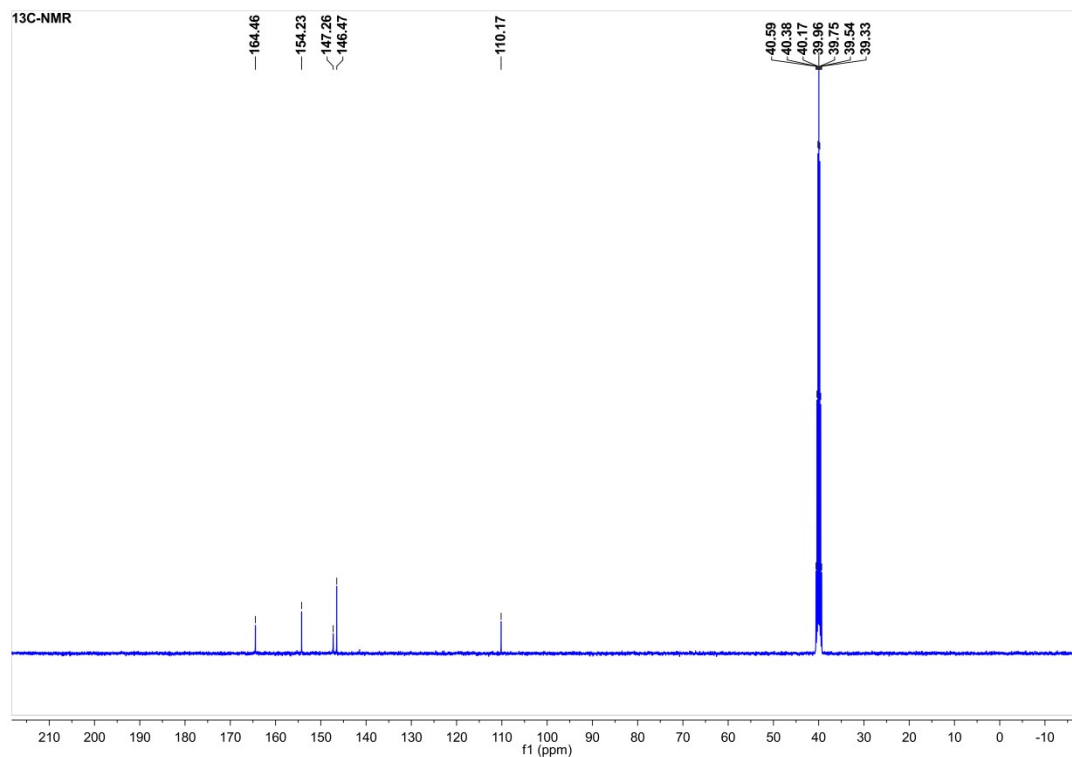


Fig. S4 ^{13}C NMR of NTTO (DMSO-d₆)

6 FT-IR spectra of NTTO

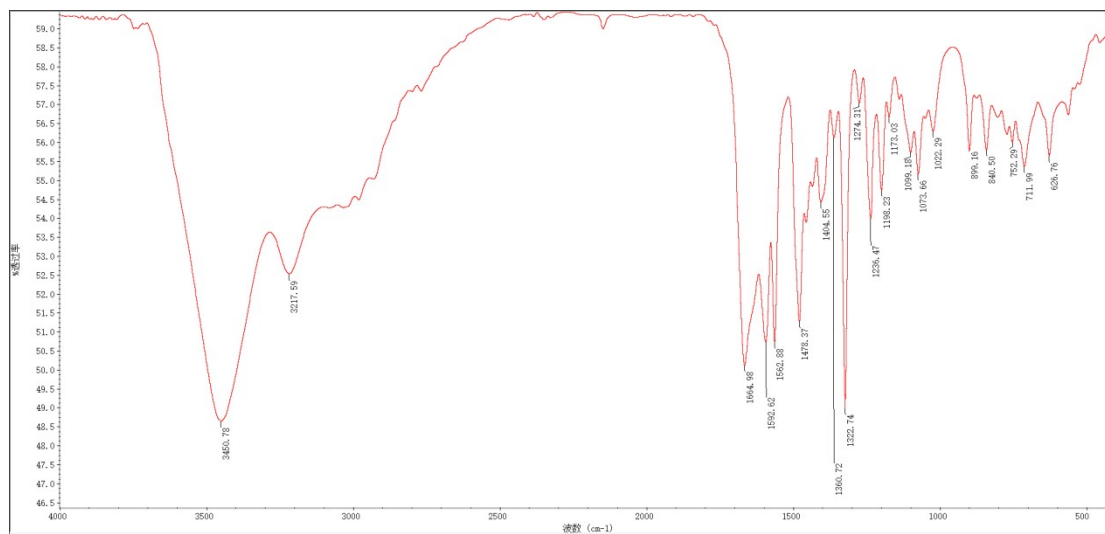


Fig. S5 FT-IR of NTTO